Proceedings of ASME Turbo Expo 2021
Turbomachinery Technical Conference and Exposition
GT2021
June 7-11, 2021, Virtual, Online

GT2021-59941

INVESTIGATION OF ADJACENT LIFTED FLAMES INTERACTION IN AN INLINE AND INCLINED MULTI-BURNER ARRANGEMENT

Mohamed Shamma*
Stefan Raphael Harth
Nikolaos Zarzalis
Dimosthenis Trimis
Engler-Bunte-Institute
Division of Combustion Technology
Karlsruhe Institute of Technology
Engler-Bunte-Ring 7, 76131 Karlsruhe, Germany
Email: mohamed.shamma@kit.edu

Sven Hoffmann
Rainer Koch
Hans-Jörg Bauer
Institute of Thermal Turbomachinery
Karlsruhe Institute of Technology
Karlsruhe, Germany

Leonardo Langone
Sofia Galeotti
Antonio Andreini
Heat Transfer and Combustion group
Department of Industrial Engineering
University of Florence
Florence, Italy

ABSTRACT

The main objective of this research is to assess an innovative, low nitrogen oxides emission combustor concept, which has the potential to achieve the long term European emissions goals for aircraft engines. Lean lifted spray flames and their very low nitrogen oxides emissions are combined with an inclination of burners in annular combustor leading to a more compact combustor with superior stability range. The presented combustor concept was developed in the frame of the European research project CHAIRLIFT (Compact Helical Arranged combustoRs with lean LIFTed flames). CHAIRLIFT combustor concept is based on "low swirl" lean lifted spray flames, which features a high degree of premixing and consequently significantly reduced nitrogen oxides emissions and flashback risk compared to conventional swirl stabilized flames. In the CHAIRLIFT combustor concept, the lifted flames are combined with Short Helical Combustors arrangement to attain stable combustion by tilting the axis of the flames relative to the axis of the turbine to enhance the interaction of adjacent flames in a circumferential direction. A series of experimental tests were conducted at a multi-burner array test rig consisting of up to five modular burners at different burner inclination angles (0° and 45°), equivalence ratios, and relative air pressure drop at ambient conditions. For all investigated configurations, a remarkable high lean blow out for non-piloted burners (ϕ_{LBO} = 0.29 - 0.37), was measured. The multi-burner configurations were observed having a superior stability range in contrast to the typical decrease in stability from single to high swirl multi-burner. The unwanted flow deflection of highly swirled flames in Short Helical Combustors arrangement, could be avoided with the investigated low swirl lifted flames. Moreover, the flame chemiluminescence (OH^*) measurements were used to provide a qualitative characterization of the flame topology. Complementary numerical investigations were carried out using different numbers of burners to evaluate the effect of boundary conditions.

Nomenclature

ACARE	Advisory Council for Aviation and Research in Europe	
A	Area	[mm^2]
A_{eff}	Effective area	[mm^2]
CFD	Computational fluid dynamics	
CO_2	Carbon dioxide	
CO	Carbon monoxide	
D	Combustor width	[mm]
FN	Flow number	[kg/h/$\sqrt{\text{bar}}$]
IRZ	Inner recirculation zone	

*Address all correspondence to this author.

LBO	Lean blow out	[kg_{air}/kg_{fuel}]
LOH	Lift-off height	[mm]
LES	Large eddy simulation	
$\dot{m}_f$	Fuel flow rate	[kg/h]
NO_x	Nitrogen oxides emission (NO+NO_2)	
NGV	Nozzle Guide Vanes	
OGV	Outlet Guide Vanes	
OH^*	Exited hydroxyl radical	
ORZ	Outer recirculation zone	
P	Pressure	[bar]
PIV	Particle image velocimetry	
PVC	Precessing vortex core	
RANS	Reynolds-averaged Navier–Stokes equations	
r	Radius	[mm]
SN	Swirl number	[-]
SHC	Short Helical Combustor	
SOx	Sulphar oxides	
T	Temperature	[K]
$\overline{T}$	Mean temperature	[K]
$\overline{u}$	Time-averaged velocity	[m/s]
UHC	Unburned Hydrocarbons	
URANS	Unsteady Reynolds-averaged Navier–Stokes equations	
UV	Ultraviolet	
ϕ	Equivalence ratio	[-]
θ	Configuration inclination angle	
$\Delta P_a/P$	Air pressure drop across the nozzle	[%]
ΔP_f	Fuel inlet pressure	[bar]

MOTIVATION AND INTRODUCTION

Due to the increasing environmental awareness over the last decades, reducing pollutant emission has sparked the interest of researchers in the design of next-generation engines. Pollutant emissions in particularly from aeronautics engines represent a great public concern due to their impact on the environment at both ground and high altitude levels. The pollutants emitted by aircraft engines in different forms include NO_x (comprising NO and NO_2), Unburned Hydrocarbons (UHC), Carbon monoxide (CO), Sulphur Oxides (SO_x), and particulate matter [1]. NO_x emissions must be kept under control due to their toxicity and the danger of interaction with the ozone layer, which leads to serious consequences for human health and the environment [2, 3].

In "Flightpath 2050", the Advisory Council for Aviation and Research in Europe (ACARE) summarized the guidelines for the future regulations, requiring a drastic reduction of aircraft pollutant emissions. The ambitious goal is to cut down 75 % of CO_2 levels and 90 % of current NO_x emissions with respect to the current standards [4]. While generally CO and UHC reduction fall within the scope of maximizing combustion efficiency and reducing the fuel consumption, the main approach of reducing NO_x emissions by reducing the combustion temperature [5]. The purpose is to achieve low-temperature combustion at full power, without penalizing excessively low power operation efficiency. Lean combustion can be employed in this perspective [6], but accurate control of local temperature is required in order to contain emission levels of other pollutant species and granting the stability and safety needs of aircraft engines [3, 5]. Swirled flames are commonly employed in technical applications due to their stable behavior. The inner recirculation zone created by the vortex breakdown ensures favorable conditions in the ignition zone including transport of heat and radical species and low mean flow velocity [3]. In contrast to highly swirled flames, which typically anchor near to the nozzle exit at the inner recirculation zone, lifted flames have the potential to provide a high level of premixing within the combustor before the reaction zone. Since the mixing zone is located within the combustor, auto-ignition and flame flashback are no safety risks and would only lead to a shorter lift-off height (LOH) for the specific operating condition. The effect of the operating condition (combustor pressure, air inlet temperature, and pressure drop) on lifted swirl spray flames was investigated experimentally by Kasabov [7]. Sedlmaier [8] and Fokaides [9] also presented experimental analysis of a confined lifted low-swirl non-premixed flames with both gaseous and liquid fuels, providing a detailed description of the flame topology. Instead of using a diffusive pilot flame to stabilize the main lean flame, an operation that partially eliminates the efforts made to reduce NO_x emissions, a novel strategy is to make the different flames of an annular combustor interact in order to stabilize each other which was developed by Ariatabar et al. [10–12].

In the present work, the short helical combustor (SHC) approach is combined with the adoption of low swirl lean lifted spray flames. By joining these two innovative combustion strategies, it is targeted to develop a new combustor concept suitable to accomplish the long term targets for NO_x emission reduction (Flightpath 2050 [4]). To assess such a concept, a modular combustor was designed, which can be equipped with up to 5 burners in different arrangements. Moreover, complementary numerical investigations were performed to determine the impact of the boundary conditions, i.e. if the selected multi-burner configuration behaves similar compared to an arrangement with infinite numbers of burners (periodic boundary conditions) and thus being suitable as an experimental reference case at a laboratory scale for such burner concept.

THEORY AND COMBUSTOR CONCEPT

In this part, the main features of the lean lifted spray flames and the SHC combustor concept, which were combined for the new combustor concept, are explained. The basic idea is to apply a low swirl lifted spray flame as investigated by Kasabov [7]. This type of flame is called "lifted" since the flame is not anchored to the injector. It features a high degree of premixing due to a mixing zone within the combustor and consequently significantly reduced NO_x emissions. The main features of such

flames are also the strongly reduced risk of flashback. However, such lifted flames have the risk of a lean blowout at some operating conditions and a longer flame length compared to swirl stabilized flames for aero-engines. The conventional way to enhance the operating range is to add a pilot flame for safe operation. However, this pilot flame may produce an additional level of unwanted NO_x emissions. Thereby, piloting of the flame is achieved by the interaction with the adjacent flame in a circumferential direction within the annular combustion chamber. This requires tilting of the axis of the flames relative to the axis of the machine as depicted in Fig. 1. This design is called Short Helical Combustor (SHC). By this SHC concept, the extra pilot flame which may produce additional NO_x emissions will be avoided. Most importantly, the turning angle of the Nozzle Guide Vanes (NGV) can be reduced which results in a smaller number of NGV and hence reduced cooling air requirements. It also reduces the length of the combustor. The SHC concept was proposed earlier by some industrial inventors [13] and [14]. An issue for the application with swirl stabilized burner is an unwanted flow deflection as shown in Fig. 2 which occurs due to flow phenomena driven by swirl flow as explained by Ariatabar et al. [12]. Thus, the use of low swirl number flows as in the case of lifted flames will permit to avoid such shortcomings of the SHC concept. Furthermore, the SHC concept enables a more compact combustor and the disadvantages of the typically more longer lifted flames are counterbalanced.

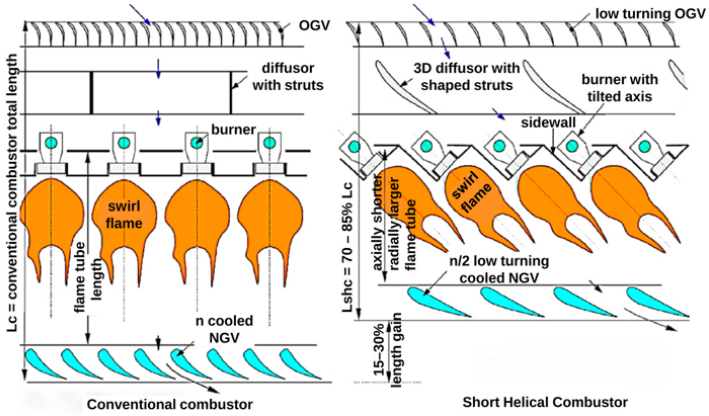

FIGURE 1: SCHEMATIC PRINCIPLE OF THE SHORT HELICAL COMBUSTOR CONCEPT [10].

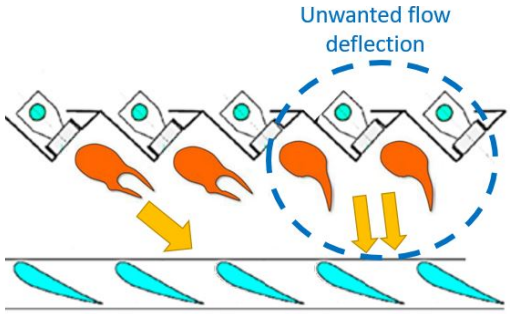

FIGURE 2: DEFLECTION OF THE FLOW BACK TOWARDS THE MACHINE AXIS.

EXPERIMENTAL SET-UP

Combustion facility and operating conditions

The experimental investigations was carried out on a multi-burner array test rig consists of up to five modular burners. The test rig is designed to operate at ambient pressure. The most important feature of the design is the flexibility of changing the inclination angle (or the vertical distance between the burners) which allows operating the test rig at inline (0°) and inclined (45°) configuration as shown in Fig. 3, in order to study the effect of burner inclination on the characteristics of the flame.

Each burner has a base plate in the combustor with a square cross-section of 100 mm x 100 mm and a combustor height of 300 mm relative to each nozzle exit as shown schematically in Fig. 4. The air plenum for each nozzle has an inner diameter of 68 mm and 435 mm in length and includes a flow straightener plate used to enhance symmetry to the inlet velocity profiles. Combustion takes place in the combined chamber of the burners array, where the adjacent flames are free to interact. Flame fused quartz glass (with a percentage of SiO_2 of $\geq 99.98\%$) windows delimit the combustion chamber, allowing wide optical access (174 x 302 mm^2) to the interaction regions of each two neighboring flames. The exhaust of the combustion chamber is open to ambient pressure with three different outlet configurations, as described in the next section.

Lifted flames are obtained using a particular air-blast nozzle with an effective area of A_{eff} = 319 mm^2 (which is already on a realistic geometrical scale for aero-engines similar to that used in previous studies by Kasabov [7]). The investigated nozzle consists of four parts; (1) Diffuser, (2) Secondary swirler, (3) Primary swirler, and (4) Inlet as shown in Fig. 5. The primary swirler consists of eight tangentially inclined vanes and the vane trailing-edges are at an angle of 45° relative to the tube axis resulting in a swirl number SN = 0.76. The secondary swirler has twelve straight vanes with zero trailing angle and zero swirl number.

To mimic real conditions of an aircraft engine jet A1 is employed as fuel and applied to the inner wall of the primary swirler by means of a hollow cone pressure atomizer located axially at the center of each burner (No. 5 in Fig. 5). Identical atomizers with 70° hollow cone angle, and flow number (FN) of 0.74 are

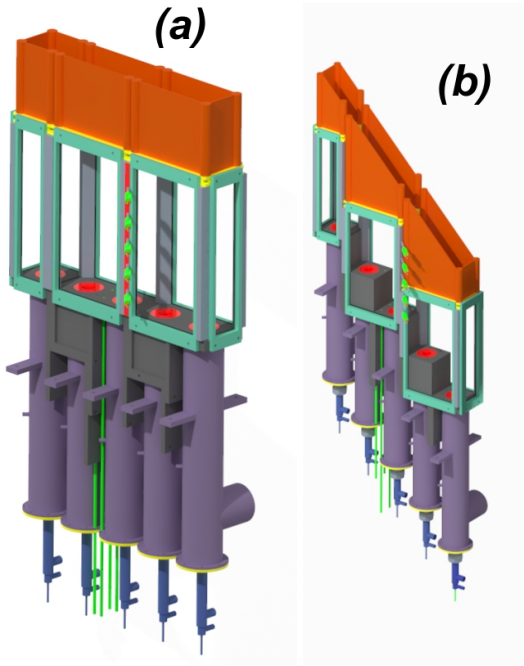

FIGURE 3: SCHEMATIC OF MODULAR BURNER ARRAY AT DIFFERENT INCLINATION ANGLE; WHERE (a) IN-LINE CASE ($\theta = 0°$) AND (b) INCLINED CASE ($\theta = 45°$).

located axially at the center of each burner. The flow number is defined as follows:

$$FN = \frac{\dot{m}_f}{\sqrt{\Delta P_f}}, \qquad \left[\frac{\mathrm{kg/h}}{\sqrt{\mathrm{bar}}}\right] \tag{1}$$

The atomization process through the selected nozzle occurs due to two consecutive atomization steps; at first a pressure swirl atomization process by a hollow cone pressure swirl atomizer, which sprays fuel forming a fuel film at the primary swirler lip. The formed fuel film at the atomizing edge is then disintegrating into smaller droplets at the shear layer between primary and secondary air flow (airblast atomization). The jet A1 fuel is inserted into the atomizer through a water-cooled fuel feeding lance (No. 6 in Fig. 5) to avoid fuel coking at the atomizer tip. Fuel mass flow rates are controlled independently for each burner, and the total flow rate is measured with Coriolis flowmeter with an accuracy of 0.5 % and pressure sensors with 1.5 % accuracy to evaluate the fuel flow rate in every burner.

The total airflow rate is measured with a thermal mass flow meter with an accuracy of 1 %. The equal distribution of air to each burner was reached by an air distributor followed by air supply lines to each burner with the same length and shape. This test campaign was performed at different operating conditions that are illustrated in table 1.

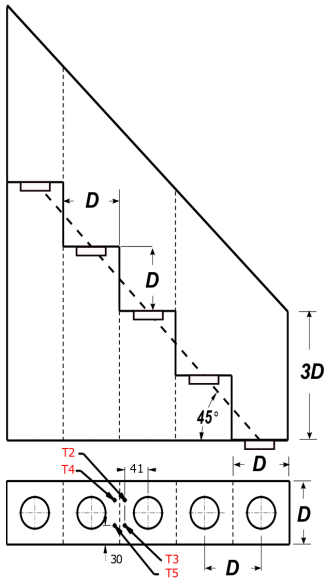

FIGURE 4: SCHEMATIC OF THE INCLINED BURNER ARRAY FROM FRONT AND TOP VIEW, WHERE: (T_2-T_5) ARE THE AXIAL TEMPERATURE AT DIFFERENT POSITIONS.

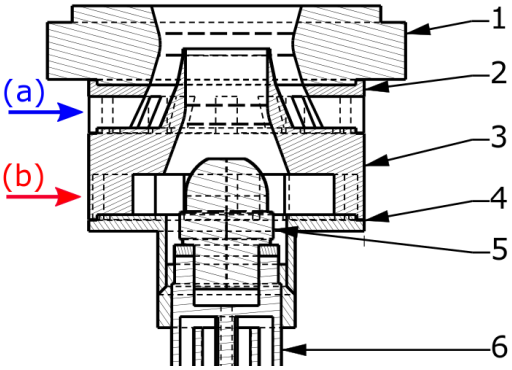

FIGURE 5: SCHEME OF THE INVESTIGATED NOZZLE TYPE, WHERE: (1) DIFFUSER, (2) SECONDARY SWIRLER, (3) PRIMARY SWIRLER, (4) INLET, (5) ATOMIZER, (6) FUEL FEEDING LANCE, (a) SECONDARY AIR AND (b) PRIMARY AIR.

Measurement techniques

Temperature measurements are performed with S-type thermocouples. Thermocouples are positioned at different positions at the test rig array to allow measuring the flame and exhaust temperature at different locations. The flame structure and the lift-off height was captured by LaVision High-Speed Star5 camera with 1024 × 1024 pixel resolution up to 5.4 kHz with a 105 mm Nikon UV lens coupled with image intensifier (LaVision High-Speed IRO) and a 307 nm ± 10 nm band pass filter.

TABLE 1: OPERATING CONDITIONS.

Parameter	Inline	Inclined
Configuration angle	0°	45°
Temperature	290 K	
Effective area of each nozzle	319 mm^2	
Air pressure drop across the nozzle	1 % - 4 %	
Equivalence ratio (ϕ)	0.39 - 0.53	

RESULTS AND DISCUSSION

Outlet configuration

For inclined configuration, the flow was observed to tilt towards the higher burner and forming a recirculation zone downstream the first two burners at the combustor outlet. Ambient air enters the combustor and is altering the global stoichiometric ratio. Thus, preventing air intake from ambient is essential to avoid unrealistic boundary conditions for a laboratory scale reference case with limited number of burners. To address this issue, two solutions were proposed: firstly by blocking the outlet of the first two burners as shown in Fig. (6-b), while the second is by using an outlet contraction as shown in Fig. (6-c).

Figure (7) shows a comparison of the temperature field at the outlet of the three different configurations. The temperature was measured using five S-type thermocouples moving in parallel (y) and normal (x) direction obtaining a temperature grid with 1 cm cell length. From Fig. (7-a) it can be observed that for the open outlet case, the temperature distribution is not uniform, because of the cold air recirculation for the lower burners and heat accumulation at the higher burner. However for both (7-b) and (7-c) the recirculation zone at the outlet was significantly decreased, thus providing a more uniform temperature distribution at the outlet. The configuration (b) with the partly blocking of the outlet has the disadvantage, that the outlet flow is forced in a certain direction dependent on the size of the outlet, which is difficult to select without knowing results from e.g. an annular combustor reference case. The case (c) with outlet contraction was selected for more detailed studies as it is more realistic compared to the later application and does not require a pre-knowledge on the flow angles at the outlet.

Flame stability

A large stability range is essential for safety and has direct impact on the pollutant emissions since it allows to operate the combustor at low combustion temperatures and related low NO_x emissions for most cycle conditions. In this work, the lean blowout (LBO) point is defined at the extinguishing point of the flame.

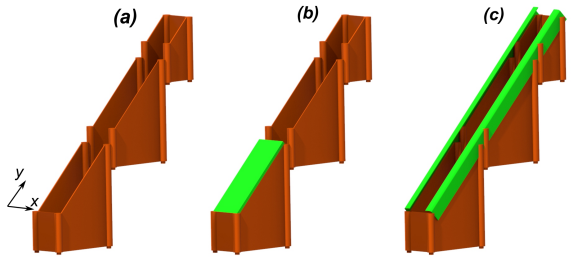

FIGURE 6: DIFFERENT OUTLET CONFIGURATION APPLIED TO THE INCLINED CASE.

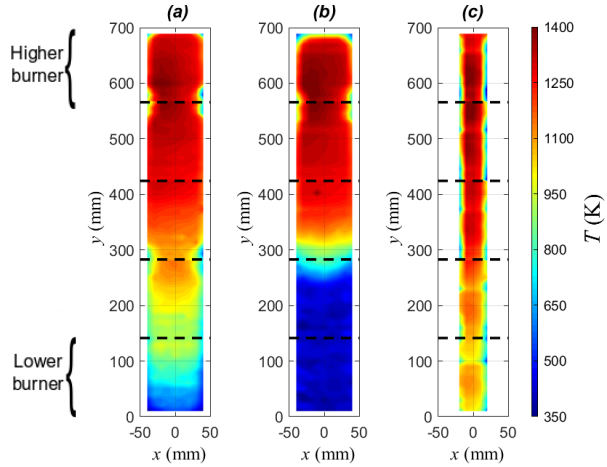

FIGURE 7: TEMPERATURE FIELD AT DIFFERENT OUTLET CONFIGURATIONS FOR INCLINED CASE AT 3% PRESSURE DROP AND 0.47 EQUIVALENCE RATIO, WHERE: CASE (A) OPEN OUTLET, CASE (B) PARTIALLY BLOCKED OUTLET, AND CASE (C) CONTRACTED OUTLET, THE DOTTED LINE REPRESENTS THE EDGE OF EACH BURNER.

The LBO measurements are performed starting from stable conditions, that is maintained for a sufficient time, and then reducing the fuel flow rate, while the airflow rate is kept constant until the flame blows out. Two types of multi-burner configuration (Inclined and Inline) were employed in the experiment and compared to a single dome rectangular confined combustor where the last burner was operated separately in confined configuration. The contracted outlet was adopted only for the inclined case to avoid the outlet vortex as explained however the inline case with open outlet was used since no outlet vortex was observed.

For the inclined configuration, the first burner (lowest) was operated 8 % more fuel rich to avoid an earlier lean blow compared to the last (highest burner). As shown in Fig. 8 The sta-

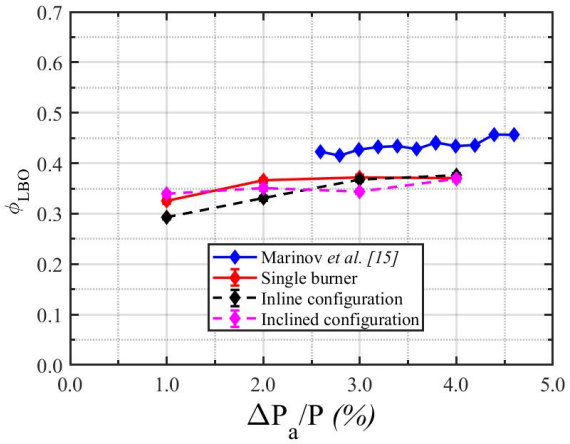

FIGURE 8: LEAN BLOW OUT LIMITS FOR DIFFERENT BURNER CONFIGURATIONS.

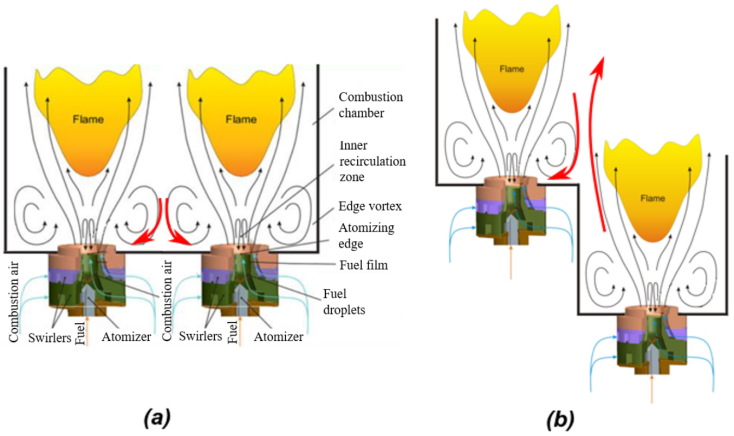

FIGURE 9: PRINCIPLE OF FLAME INTERACTION AT DIFFERENT LEVELS (REPRODUCED FROM SINGLE BURNER SCHEME [7]).

bility of the single burner with lifted flame is surprisingly high compared to lean flames with high swirl, e.g. Marinov et al. [15] which was operated even at higher inlet air temperature (540 K). A possible reason is that the lifted flames enable evaporation of fuel droplets within the combustor also at low air inlet temperatures due to the recirculation of hot exhaust gases in the outer recirculation zone (ORZ). This is indicated by the observed quite blue flame, which is not typical for JET-A1 fueled flames at air inlet temperatures of 290 K. Another potential reasons could be, that for the lower air inlet temperatures, less pre-evaporation could occur within the nozzle and the jet exit and more droplet are traveling outwards and make it locally rich at the shear layer zone between the inner recirculation zone (IRZ) and ORZ where the swirl flames stabilize.

Also from the experimental results, the multi-burner configurations were observed having a superior stability range in contrast to the typical decrease in stability from single to high swirl multi-burner investigated by Kraus [16] for gaseous fuel and Dolan [17] for liquid fuel. Considering that, the flame roots of the inclined configuration are stabilized by the hot exhaust gases of the lower flames, it is remarkable, that there is not much difference in stability between the inline and inclined cases. A potential explanation is related to the flow interaction, which is schematically shown in Fig. 9. For the inline configuration, the ORZ may enhance each other due to the same flow direction at the position as indicated by a red arrow in Fig. (9-a). On contrary, it is possible that for the investigated inclined configuration, that the axial momentum of exhaust gases of the lower flame decreases the amount of recirculated air in ORZ of the upper burner due to opposing velocity vectors as indicated in Fig. (9-b). In essence, the flow interaction in the inclined configuration has the advantages of exchanging hot exhaust gases (nearly completely burnt) to the ORZ and flame root of the neighboring burner, but the potential disadvantage of affecting the recirculated flow. These opposite impacts could lead to the similar stability of the inclined to the inline configuration, which both exhibit superior lean blowout limits compared to the typical highly swirled lean burner without pilot flame.

Reaction zone

Lift-off height The lift-off height (LOH) is defined as the distance between the burner dome and the flame reaction zone. In this study, the lift-off height was determined based on high-speed OH^*chemiluminescence measurements and defined as the distance between the nozzle exit and the horizontal line upstream of which 10 % of the total chemiluminescence intensity is present. As explained by Lauer et al. [18] The chemiluminescence is not a perfectly a suitable tool for representing the heat release distribution as it could be biased by many parameters of the reacting flow (i.e. turbulence, strain rates, CO_2^* concentration). Therefore, the shape of the whole reaction zone was chosen to define the lift-off height instead of absolute values (i.e maximum value) to minimize potential deviations according to the above mentioned flow parameters.

The following procedure has been adopted for the lift-off height calculation. First of all, the chemiluminescence intensity of each pixel is averaged over 2000 images (with 90 000 ns gate timing) that were recorded for every test condition. Lift-off position is set where the cumulative of the horizontally averaged intensity first reaches the threshold value. The threshold value for the lift-off height definition is set to 10 % of the sum of all pixels for the specific operating point [7] .

In this section, LOH is quantified at a constant air inlet temperature (290 K) for various conditions (pressure drop, equivalence ratio, and configuration) as indicated in Fig. 10.

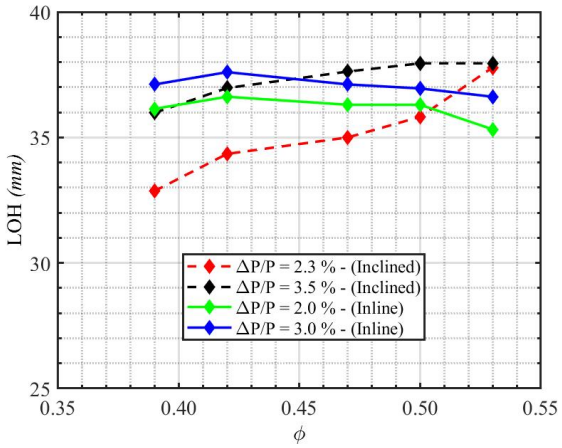

FIGURE 10: INFLUENCE OF PRESSURE DROP ON LOH FOR DIFFERENT CONFIGURATION.

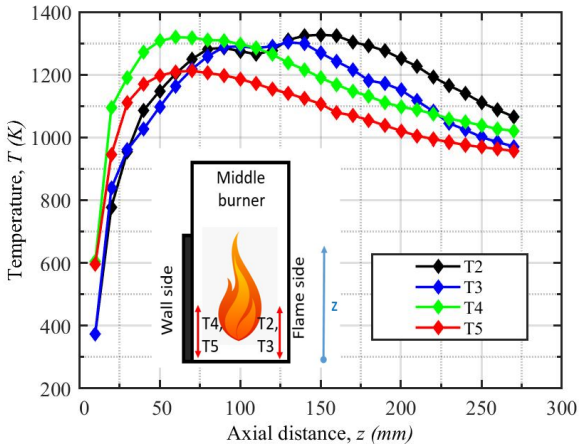

FIGURE 11: AXIAL TEMPERATURE MEASUREMENT FOR INCLINED CASE AT DIFFERENT LOCATIONS AT 3% PRESSURE DROP AND 0.47 EQUIVALENCE RATIO.

The dashed lines identify the measurements of incline configuration and the solid lines depict the measurements for the inline configuration. For the inclined burner configuration, the calculated lift-off height is decreasing with increasing equivalence ratio. A potential reason is, that part of fresh gas of the burner is exchanged with burnt gases from zone b from the neighboring burner as marked in Fig. 12.

These fresh gases are burnt more downstream and are not counted for the lift off height calculation since they spread to the next burner (only red dashed box in Fig. 12, $\phi = 0.47$, is used for the LOH calculation). At the same time, in zone a, the burner could receive fresh gases from the neighboring burner, which is allocated more upstream and thus leading to this increase in calculated lift off height. Figure 13 shows that the inline array has approximately the same shape for all the equivalence ratio variation and the flames are nearly symmetric around the nozzle axis. The slight asymmetry could be related to the rods for the windows. For the inclined case as shown in Fig. 12, It was noted that the flames are less intense at the side facing the lower flame. The reason could be, that this side receives already burnt gases from the neighboring burner by turbulent mixing processes and delivers part of the fresh gas to the neighbor flame. This would also explain, why the measured axial temperature distribution (Fig. 11) at this less intense flame side is higher compared to the other side. However, the flame branch near to the higher burner is stronger due to fuel exchange with this higher flame compared to exhaust gas exchange with lower flame. The same observation was confirmed with axial temperature as shown in Fig.11.

NUMERICAL INVESTIGATION

In this section, the results of the numerical investigation of the inclined multi-burner arrangement supporting the experimental study are presented. The objective of the flow predictions is to prove that the boundary conditions of the combustor test rig reflect an appropriate setup for studying the lifted flame in the staggered SHC arrangement at laboratory scale. Thereby, special emphasis is put on the interaction between the low-swirl flows in adjacent sectors. Furthermore, it will be demonstrated that five sectors are sufficient to mimic a periodic arrangement of an annular concept limiting the impact of confining combustor walls.

The CFD simulations are performed using a pressure based solver of the numerical toolbox OpenFOAM 7. In the numerical setup employed in this work, the nozzle which is used in the experimental study imposing the swirl of the flow (Fig. 5) is omitted. Instead, specific profiles for each velocity component are prescribed at the circular inlet patch of the computational domain. In a RANS framework, this helps to reduce the complexity of the problem. However, to ensure that the typical flow pattern of the low-swirl flow is established downstream the nozzle, this approach is to be validated.

Validation of the numerical model

In Fig. 14, the computational domain of the validation study is shown. It features the geometry of a cylindrical flame tube used in a previous experimental campaign [8, 19]. The circular inlet and outlet patches are located at the bottom and the top of the combustor respectively. By using a contraction at the outlet, backflow is prevented. The domain is discretized by a block-structured mesh consisting of approximately 2 million hexahedral elements.

The profiles of each directional velocity component imposed by the boundary condition at the inlet are illustrated in Fig. 14. The velocity profiles were obtained from isothermal LES predictions of the flow through the realistic swirl nozzle at ambient

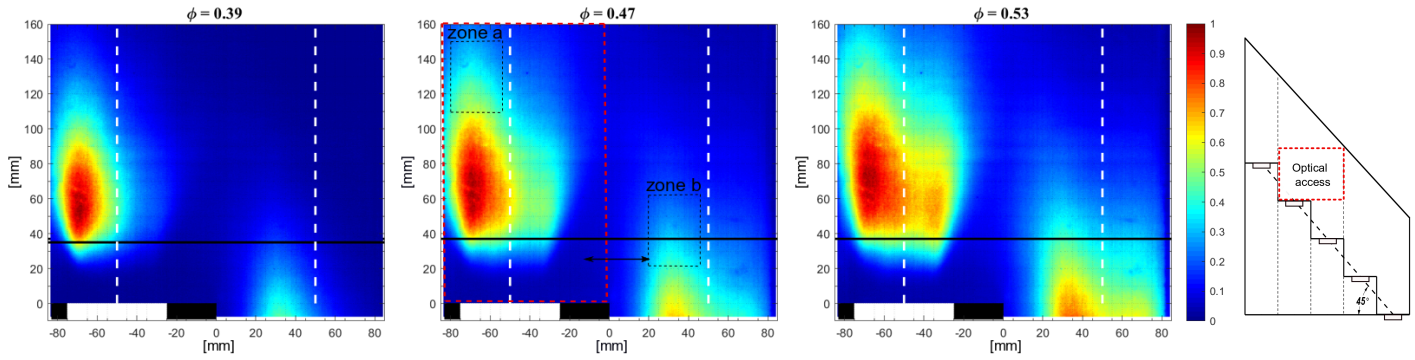

FIGURE 12: MEASUREMENTS OF NORMALIZED INTENSITY OF OH* CHEMILUMINESCENCE NORMALIZED TO EACH IMAGE MAXIMUM FOR THE INCLINED CONFIGURATION AT 3 % PRESSURE DROP AND DIFFERENT EQUIVALENCE RATIO, WHERE: THE BLACK HORIZONTAL LINES MARK THE LOH AND THE VERTICAL WHITE LINES ARE THE NOZZLES AXES.

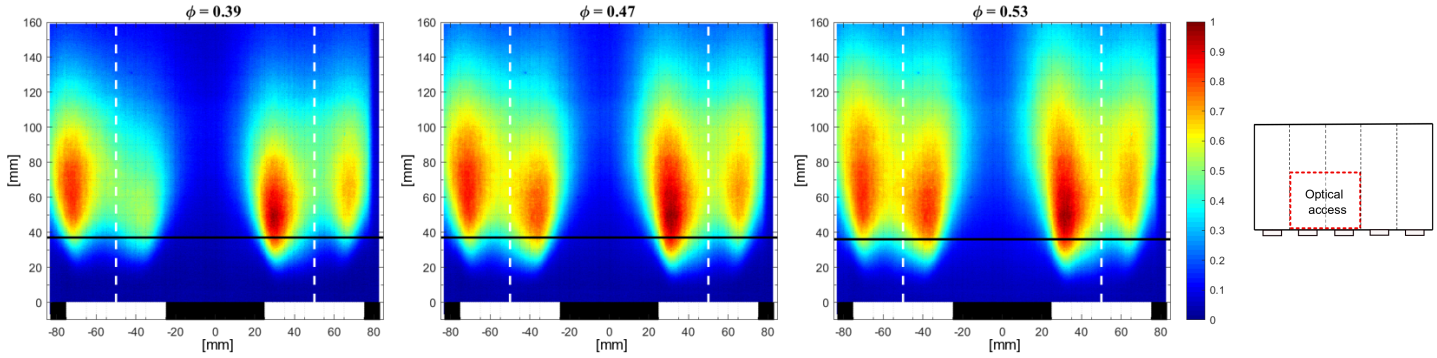

FIGURE 13: MEASUREMENTS OF NORMALIZED INTENSITY OF OH* CHEMILUMINESCENCE NORMALIZED TO EACH IMAGE MAXIMUM FOR THE INLINE CONFIGURATION AT 3 % PRESSURE DROP AND DIFFERENT EQUIVALENCE RATIO, WHERE: THE BLACK HORIZONTAL LINES MARK THE LOH LENGTH AND THE VERTICAL WHITE LINES ARE THE NOZZLES AXES.

pressure performed by Langone et al. [20]. The relative pressure drop across the injector was 3 %. The profiles representing time-averaged fields were extracted at the end section of the nozzle which denotes the transition between the nozzle and the flame tube. In a preliminary study related to this work, it was found that a turbulence kinetic energy of 12 % prescribed at the inlet gives the best fit to the flow field of the experiment.

To account for the transient behavior of the flow, the unsteady RANS method is employed. The total physical time captured by the simulation is 660 ms including 360 ms used for time-averaging. Turbulence is modeled by using the renormalization group (RNG) k-ε model [21]. Spatial derivatives are discretized by second order schemes. For the temporal discretization, a second order time implicit scheme is employed. At solid walls, adiabatic no-slip conditions are enforced.

The comparison of time-averaged profiles of the axial and tangential velocity components between the numerical prediction and experiment [19] is presented in Fig. 15. At three designated axial positions downstream the inlet, the profiles of the simulation are extracted and circumferentially averaged in space. The profiles are in good agreement with experimental data with a small deviation further downstream. The distribution of axial velocity in radial direction of the flame tube exhibits the typical flow pattern of the nozzle characterized by a low-swirl jet. Due to the low swirl number of the flow, which is well below 0.4, vortex breakdown causing a large IRZ does not occur [22]. In contrast, the IRZ related to this type of injector shows a small dimension in axial and radial direction. However, this is not entirely captured by the simulation. The lean lifted flame is mainly stabilized by outer recirculation zones bringing back reactive radicals to promote fuel-air mixing and to constantly ignite the flame. The outer

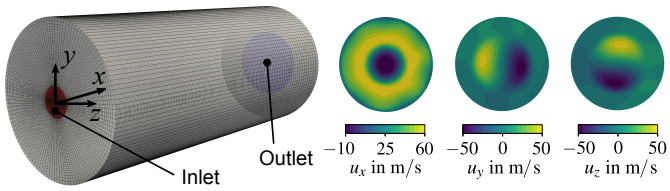

FIGURE 14: COMPUTATIONAL DOMAIN OF THE FLAME TUBE (LEFT) AND VELOCITY PROFILES AT THE INLET (RIGHT).

recirculation zone is well reproduced, since slightly negative axial velocities at higher radii are found. In addition, the second velocity peak in the tangential profiles, which is associated with the helical flow structure of recirculating fluid, is predicted correctly.

For studying the transient behavior of the flow, a time sequence of the precessing jet is shown in Fig. 16. Thereby, three different snapshots of a time interval of 120 ms are visualized by a contour of constant axial velocity. Jet precession is different to the precessing vortex core (PVC) and is related to very low swirl numbers [23]. Sedlmaier [19] observed in experimental investigations a rotational movement of the isothermal flow around the burner axis with a frequency of 3 – 4 Hz. This complex precessing flow field can be reproduced with the present numerical setup based on the URANS method.

The proposed approach of omitting the nozzle geometry and instead imposing highly resolved velocity patterns at the inlet patch enables the prediction of the realistic flow field of this particular type of nozzle. In a similar approach, Ariatabar et al. [10] used tangential velocity profiles of rigid-body vortices at the inlet modeled as a two-slots coaxial swirler in their fundamental studies of the SHC concept.

To conclude, both the time-averaged velocity profiles downstream the nozzle and the transient phenomenon of jet precession are in good agreement with experimental data. Hence, the numerical setup can be considered as suitable and will be used subsequently for the multi-burner arrangement.

Numerical setup of the multi-burner arrangement

In this section, the setup of the flow analysis of the inclined combustor configuration featuring a tilting angle of 45° is presented. In Fig. 17, the generic computational domain which is derived from the geometry of the experimental burner array as shown in Fig. 3 is presented. The nozzle of this study results from a direct scale-up of the nozzle used by Sedlmaier et al. [8, 19] which preserves geometric similarity. As outlined before, the swirl nozzles are omitted in numerical simulations. Since the nozzle used in the test rig of this study ($A_{\text{eff}} = 319\,\text{mm}^2$) is larger compared to that used by Sedlmaier et. al [8, 19] ($A_{\text{eff}} = 131\,\text{mm}^2$), the circular inlet patches of the domain are

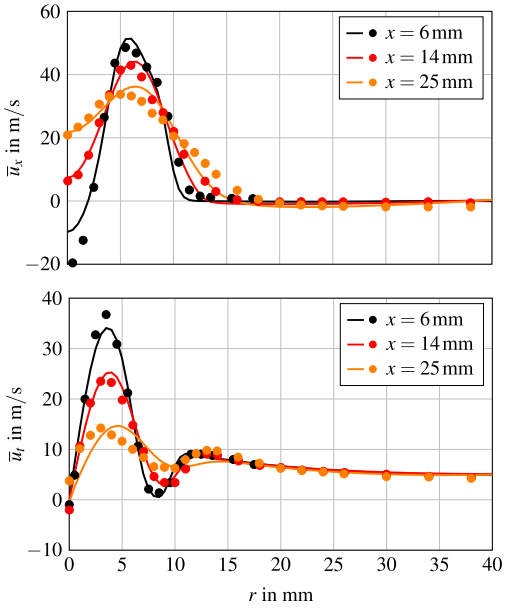

FIGURE 15: AXIAL (TOP) AND TANGENTIAL (BOTTOM) TIME-AVERAGED VELOCITY COMPONENTS OF EXPERIMENT (●) AND SIMULATION (—).

scaled up according to the ratio of the nozzle diameters. Additionally, the velocity profiles prescribed at the inlets (Fig. 14) are scaled to account for the higher discharge coefficient of the larger nozzle. Consequently, the correct air mass flux according to the larger nozzle is set. By imposing the same relative pressure drop across the injectors, Mach number similarity is ensured as well. Hence, it is expected that the velocity profiles of the similar injector nozzles are qualitatively equal.

The temperature at the inlet is the ambient temperature of 290 K. For the case of backflow at the outlet, ambient temperature is prescribed for inflowing air. The operating pressure of $p = 1\,\text{bar}$ is imposed at the outlet. Adiabatic no-slip conditions are enforced at the combustor walls. The computational grid consists of about 14 million elements, mostly hexahedral cells, featuring refinement zones close to the inlets. For mesh generation, an efficient octree algorithm is applied.

Results of a preliminary study revealed, that no significant transient phenomena related to jet precession is present. This is attributed to missing confinements in the multi-burner arrangement in comparison to the enclosed flow situation of the single flame tube. Consequently, the RANS method providing the steady-state solution is used. Furthermore, it is assumed that for the present combustor design the inlet velocity profiles of the confined case are valid, since only little changes of the pressure field attributed to a reduced confinement will not have much of an upstream effect altering the high-momentum low-swirl jet.

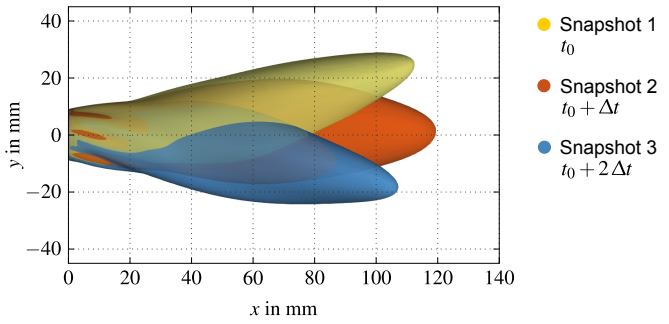

FIGURE 16: TIME SEQUENCE OF THE PRECESSING JET AT THREE SNAPSHOTS FOR $\Delta t = 120\,\text{ms}$. VISUALIZATION BY CONTOUR SURFACE OF CONSTANT AXIAL VELOCITY.

Therefore, for all flow predictions, the validated numerical model presented previously is employed.

By using heat sources in the simulations (Fig. 17), the heat release of the flames and, hence, the thermal expansion of the flow is simulated. Resolving chemical reactions of the low-swirl lifted flame in a confining flame tube by LES predictions is addressed by only few studies [19, 20, 24]. These studies demonstrate that capturing characteristic effects governing the structure of this particular flame type is challenging and that enormous computational effort is required. The heat sources selected in the present work provide a thermal power of each 35 kW which is uniformly distributed. The thermal power of the heat sources is adjusted to match the temperature increase of the flow in the experiment. Therefore, convective and radiative heat losses of the combustor are taken into account implicitly in the numerical predictions. Furthermore, the heat sources are of a conical shape which mimics the shape of the real flame to first order of accuracy [8]. Since a large temperature range has to be captured affecting the fluid properties, the temperature dependence of heat capacity and viscosity are taken into account.

In the following section, the results of the flow analysis of two variants of outlet configuration are presented (Fig. 6): without outlet contraction (a) and with partially blockage at the combustor liners (c).

Flow analysis

The temperature fields of both variants in the circumferential mid-plane are reported in Fig. 18. Furthermore, streamlines of the velocity field in this plane are shown. In both cases investigated, the flow is deflected in lateral direction towards the right combustor wall. The flow deflection is attributed to an asymmetric pressure field in the vicinity of the sidewalls of the staggered dome caused by the Coandă effect. The mechanism is elucidated in detail by Hoffmann et al. [25]. Due to the deflection, a large backflow zone B at the outlet of the first two sectors is established for variant (a). Accordingly, cold ambient air enters the combustor altering the global air-fuel ratio and leading to unrealistic conditions. This finding emphasizes the requirement of an outlet contraction of the combustor test rig studied in the present work to address backflow issues.

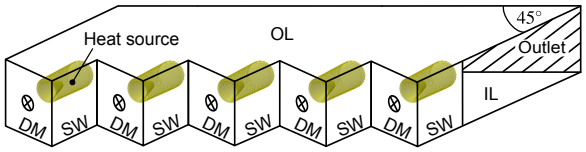

FIGURE 17: COMPUTATIONAL DOMAIN AND HEAT SOURCES OF THE INCLINED MULTI-BURNER ARRANGEMENT. DM: DOME, SW: SIDEWALL, OL: OUTER LINER, IL: INNER LINER.

The flow field of variant (c) characterized by a partially blocked outlet still exhibits the flow deflection resulting in a vortex V located close to the outlet of the first sector. However, backflow at the outlet does not occur since the flow is contracted and accelerated towards the circumferential mid-plane. This effect is indicated by the temperature contours not showing an intrusion of cold air at the outlet region which highlights the remedy by the contraction. Please note that the maximum temperature is relatively high compared to a lean flame. This yields a higher thermal expansion due to the decrease in density. However, this effect is expected to be negligible, since it only occurs locally and the characteristics of the global flow field is not affected. In this regard, the thermal power of the heat sources are determined to reflect a realistic overall temperature increase of the flow as quantified by the mean temperature at the outlet.

In Fig. 19, the temperature fields at the outlet plane of the two variants are illustrated. On the one hand, the large zone of backflow is observable as indicated by ambient temperature of 290 K for the unblocked variant (a). On the other hand, variant (c) shows a homogeneous temperature pattern across the reduced outlet with no indication of backflow. Hence, the mean temperature $\overline{T}$ which features a mass flux weighted average is higher for the latter variant and closer to the adiabatic flame temperature. Comparing these results to experimentally measured temperature fields (Fig. 7), good agreement can be endorsed bearing in mind the low-level complexity of the numerical model omitting the swirl nozzle and applying heat sources as flame replacements.

The temperature field and the streamlines of the flow in a tilted single sector including outlet contraction are shown in Fig. 20. By using translational cyclic boundary conditions indicated by dashed lines, the interaction of the low-swirl flows of adjacent combustor sectors is taken into account. In comparison to the flow in the middle sector of the multi-burner arrangement (Fig. 18), the structure of the flames is of similar shape. Hence,

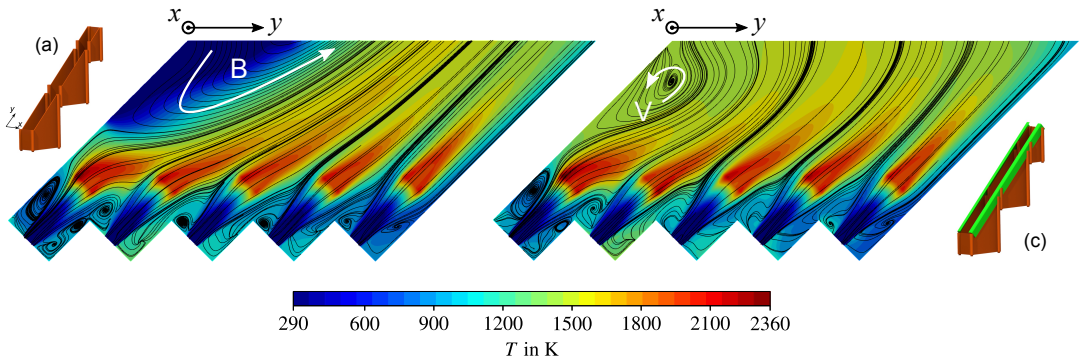

FIGURE 18: TEMPERATURE FIELDS AND STREAMLINES IN CIRCUMFERENTIAL MID-PLANE WITHOUT CONTRACTION (VARIANT (A), LEFT) AND WITH BLOCKAGE (VARIANT (C), RIGHT). ARROWS INDICATE THE FLOW DIRECTION.

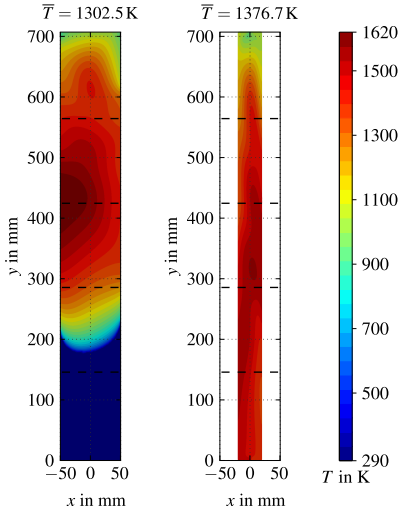

FIGURE 19: TEMPERATURE FIELDS AT THE OUTLET PLANE WITHOUT CONTRACTION (VARIANT (A), LEFT) AND WITH BLOCKAGE (VARIANT (C), RIGHT).

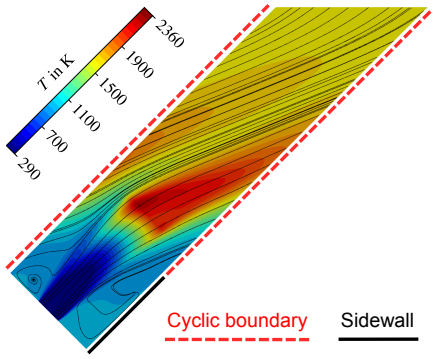

FIGURE 20: TEMPERATURE FIELD AND STREAMLINES IN CIRCUMFERENTIAL MID-PLANE OF PERIODIC CASE.

the middle sector is suited for the experimental measurements of the multi-burner array, since the impact of confining combustor walls is limited yielding an almost periodic configuration.

CONCLUSIONS AND OUTLOOK

In this work a qualitative assessment of an innovative combustor concept called CHAIRLIFT combustor was presented experimentally and numerically. This CHAIRLIFT combustor concept combines two main features:

- Short helical combustor.
- Low swirl-lean-lifted flames for liquid fuels.

From the numerical investigation, it was demonstrated that the simplified numerical model is capable of reproducing characteristic flow phenomena related to this type of low-swirl nozzle. The study of the low-swirl flow within the inclined multi-burner arrangement confirmed that by applying an outlet contraction preventing backflow of ambient air, the boundary conditions reflect an appropriate setup for experimental investigations.

The experimental investigation showed that the undesired flow deflection of swirled flames in SHC arrangement was avoided by using low swirl, the same observations was also confirmed from the numerical simulations.

For all investigated configurations, a remarkable high lean blow out for non-piloted burners (ϕ_{LBO} = 0.29 - 0.37), was measured. The multi-burner configurations were observed having a superior stability range in contrast to the typical decrease in stability from single to high swirl multi-burner investigated by Kraus [16] for gaseous fuel and Dolan [17] for liquid fuel. This could be explained by the transfer of hot exhaust gas from the neighboring burner to the flame root of the next burner for the inclined configuration and due to recirculation zones enhancement in inline configuration, which is essential for the stabilization of the lifted flames.

In the next steps of this research, Particle Image Velocimetry (PIV) measurements will be performed to obtain the velocity fields at the flame interaction region, which will help to improve the understanding of this flame stability behavior and to validate more detailed numerical simulations. Moreover, exhaust gas fields will be measured to determine the combustion progress in the flame interaction zone and the overall pollutant emission performance. In future work related to the numerical investigation of the presented combustor concept, the shape and the distribution of heat release of the heat sources will be optimized.

ACKNOWLEDGMENT

This project has received funding from the Clean Sky 2 Joint Undertaking (JU) under grant agreement No. 831881 (CHAiRLIFT). The JU receives support from the European Union's Horizon 2020 research and innovation programme and the Clean Sky 2 JU members other than the Union. The numerical computations were performed on the high performance computing cluster bwUni-Cluster at the Karlsruhe Institute of Technology. The HPC resource bwUniCluster is funded by the Ministry of Science, Research and the Arts Baden Württemberg and the DFG ("Deutsche Forschungsgemeinschaft"). The authors acknowledge support by the state of Baden-Württemberg through bwHPC. The authors would like also to thank the German Research Foundation (DFG) for the financial support of measuring instruments within the HBFG program (INST 121384/178-1 FUGG).

References

[1] Liu, Yize, Sun, Xiaoxiao, Sethi, Vishal, Nalianda, Devaiah, Li, Yi-Guang and Wang, Lu. "Review of modern low emissions combustion technologies for aero gas turbine engines." *Progress in Aerospace Sciences* Vol. 94 (2017): pp. 12–45. DOI 10.1016/j.paerosci.2017.08.001.

[2] Folinsbee, Lawrence J. "Human health effects of air pollution." *Environmental health perspectives* Vol. 100 (1993): pp. 45–56. DOI 10.2307/3431520.

[3] Lefebvre, Arthur H. "Gas turbine combustion." .

[4] Kallas, Siim and Geoghegan-Quinn, Máire. "Flightpath 2050: Europe's Vision for Aviation: Report of the High Level Group on Aviation Research." *European Union* Vol. 100 (2011): pp. 1–24. DOI 10.2777/50266.

[5] Lieuwen, Tim C and Yang, Vigor. *Gas turbine emissions*. Vol. 38. Cambridge university press (2013).

[6] Law, Chung K. *Combustion physics*. Cambridge university press (2010).

[7] Kasabov, Plamen, Zarzalis, Nikolaos and Habisreuther, Peter. "Experimental study on lifted flames operated with liquid kerosene at elevated pressure and stabilized by outer recirculation." *Flow, turbulence and combustion* Vol. 90 No. 3 (2013): pp. 605–619. DOI 10.1007/s10494-013-9444-1.

[8] Sedlmaier, Julia, Habisreuther, Peter, Zarzalis, Nikolaos and Jansohn, Peter. "Influence of liquid and gaseous fuel on lifted flames at elevated pressure stabilized by outer recirculation." *Turbo Expo: Power for Land, Sea, and Air* Vol. 45684. DOI 10.1115/GT2014-25823.

[9] Fokaides, Paris A, Kasabov, Plamen and Zarzalis, Nikolaos. "Experimental investigation of the stability mechanism and emissions of a lifted swirl nonpremixed flame." *Journal of engineering for gas turbines and power* Vol. 130 No. 1 (2008): pp. 011508–1–011508–9. DOI 10.1115/1.2749279.

[10] Ariatabar, Behdad, Koch, Rainer, Bauer, Hans-Jörg and Negulescu, Dimitrie. "Short helical combustor: Concept study of an innovative gas turbine combustor with angular air supply." *Journal of Engineering for Gas Turbines and Power* Vol. 138 No. 3 (2016): pp. 031503–1–031503–10. DOI 10.1115/1.4031362.

[11] Ariatabar, Behdad, Koch, Rainer and Bauer, Hans-Jörg. "Short helical combustor: Dynamic flow analysis in a combustion system with angular air supply." *Journal of Engineering for Gas Turbines and Power* Vol. 139 No. 4 (2017): pp. 041505–1–041505–8. DOI 10.1115/1.4034688.

[12] Ariatabar, Behdad, Koch, Rainer and Bauer, Hans-Jörg. "Short Helical Combustor: Flow Control in a Combustion System With Angular Air Supply." *Journal of Engineering for Gas Turbines and Power* Vol. 140 No. 3 (2018): pp. 031507–1–031507–6. DOI 10.1115/GT2017-63037.

[13] Hall, Russell S. "Spiral annular combustion chamber." (1961). US Patent 3,000,183.

[14] Schutz, Herbert, Kraupa, Werner and Termuhlen, Heinz. "Gas turbine engine with tilted burners." (1999). US Patent 5,946,902.

[15] Marinov, Svetoslav, Kern, Matthias, Zarzalis, Nikolaos, Habisreuther, Peter, Peschiulli, Antonio, Turrini, Fabio and Sara, O Nuri. "Similarity issues of kerosene and methane confined flames stabilized by swirl in regard to the weak extinction limit." *Flow, turbulence and combustion* Vol. 89 No. 1 (2012): pp. 73–95. DOI 10.1007/s10494-012-9392-1.

[16] Kraus, Christian, Harth, Stefan and Bockhorn, Henning. "Experimental investigation of combustion instabilities in lean swirl-stabilized partially-premixed flames in single- and multiple-burner setup." *International Journal of Spray and Combustion Dynamics* Vol. 8 No. 1 (2016): pp. 4–26. DOI 10.1177/1756827715627064.

[17] Dolan, Brian, Gomez, Rodrigo Villalva and Gutmark, Ephraim. "Optical measurements of interacting lean direct injection fuel nozzles with varying spacing." Vol. 56697. 2015. DOI 10.1115/gt2015-43706.

[18] Lauer, Martin and Sattelmayer, Thomas. "On the adequacy of chemiluminescence as a measure for heat release in turbulent flames with mixture gradients." *Journal of Engineering for Gas Turbines and Power* Vol. 132 No. 6 (2010): pp. 061502–1–061502–8. DOI 10.1115/1.4000126.

[19] Sedlmaier, Julia. "Numerische und experimentelle Untersuchung einer abgehobenen Flamme unter Druck." Ph.D. Thesis, Karlsruher Institut für Technologie (KIT), Karlsruhe, Germany. 2019.

[20] Langone, Leonardo, Sedlmaier, Julia, Nassini, Pier Carlo, Mazzei, Lorenzo, Harth, Stefan and Andreini, Antonio. "Numerical Modeling of Gaseous Partially Premixed Low-Swirl Lifted Flame at Elevated Pressure." *Proceedings of ASME Turbo Expo 2020: Turbomachinery Technical Conference and Exposition, Virtual, Online*. 2020. DOI 10.1115/GT2020-16305. No. GT2020-16305.

[21] Yakhot, Victor. and Smith, Leslie M. "The Renormalization Group, the ε-Expansion and Derivation of Turbulence Models." *Journal of Scientific Computing* Vol. 7 No. 1 (1992): pp. 35–61. DOI 10.1007/bf01060210.

[22] Gupta, Ashwani, Lilley, David and Syred, Nick. *Swirl flows*. Abacus Press, Tunbridge Wells, Kent (1984).

[23] Syred, Nicholas. "A review of oscillation mechanisms and the role of the precessing vortex core (PVC) in swirl combustion systems." *Progress in Energy and Combustion Science* Vol. 32 No. 2 (2006): pp. 93–161. DOI 10.1016/j.pecs.2005.10.002.

[24] Kern, Matthias, Fokaides, Paris, Habisreuther, Peter and Zarzalis, Nikolaos. "Applicability of a Flamelet and a Presumed JPDF 2-Domain-1-Step-Kinetic Turbulent Reaction Model for the Simulation of a Lifted Swirl Flame." *Proceedings of ASME Turbo Expo 2009: Power for Land, Sea, and Air, Orlando, Florida, USA*. 2009. DOI 10.1115/gt2009-59435. No. GT2009-59435.

[25] Hoffmann, Sven, Koch, Rainer and Bauer, Hans-Jörg. "Numerical Investigation of Low Swirl Flow in an Aeronautical Combustor With Angular Air Supply." *Proceedings of ASME Turbo Expo 2021: Turbomachinery Technical Conference and Exposition, Virtual, Online*. 2021. No. GT2021-59286, Accepted.